CHAPTER – 1

Introduction

1.1 Introduction

The mineral perovskite was found and named after the mineralogist from Russia, L.A. Perovski, first discovered by Gustav Rose [1] in the Ural Mountains of Russia in 1839. Perovskites general formula is ABO_3. Where A is greater than B cations, and where O is the anion. The octahedral coordination can be taken from the B ions; it can be from 3d, 4d or 5d transition metal ions. The perovskite substance composition is a large family of [compounds of mineral perovskite $CaTiO_3$-related crystal. Octahedral BX_6 derives the ABX_3 perovskite cubic structure with the A cation occupying the 12-fold coordination site formed in the center of the eight octahedral cube. The perovskite ABO_3 forms are known to be an FCC-derivative structure in which the larger A cation and oxygen together form a FCC lattice, and the smaller B cation occupies the interstitial octahedral sites. B cations closest neighbor is oxygen only, and many oxides, several of which have technological applications, display the perovskite structure. The perovskite oxide family is probably the best known oxide family, and it is also strongly skewed by mineral perovskite itself.

Skewed Perovskites, in particular the ferroelectric tetragonal form of $BaTiO_3$, have great at industrial significance for their magnetic and electrical properties. The formula ABO_3, where A is larger, occupies 8 corner positions in ideal perovskite structures, and B ions (smaller size) occupy the center position of the body and oxygen ions occupy the center of six faces. The distance A-O is $(a/\sqrt{2})$ whereas the distance B-O is equal to (a/2) where a is the parameter of the cubic unit cell. The following ionic radii relationship holds $(r_a + r_o) = \sqrt{2(r_b + r_o)}$ for an ideal structure where the atoms touch each other. Although this equation is not precisely obeyed for the deviation from the ideal

situation, Goldschmidt derived a tolerance factor (t) equation that relates to the empirical ionic radii at room temperature.

$$t = \frac{(r_a + r_b)}{\sqrt{2(r_b + r_o)}} \qquad (1.1)$$

The tolerance factor (t) describes the range of relative sizes that are stable for the perovskite structure. This structure is also found for lower values ($0.75<t<1.0$) where as unity is an ideal perovskite t. It will be a cubic structure if the tolerance factor (t) is similar to being one. Distorted perovskite structures have a tolerance factor ranging from 0.75 to 0.95 non-ferroelectric, whereas those with ≥1.0 are ferroelectric [3, 4, 5]. The compound does not crystallize in perovskite structure if the tolerance factor is less than 0.75. The $CaTiO_3$ compound was considered cubic, but it was later shown to be orthorhombic [2] in its true symmetry.

ABO_3 types perovskite can be classified into five classifications based on Cations A and B valancies and in which cations A valencies are n and m for B cations and formula as $A^{+n}B^{+m}$ O_3 [6]. To order to maintain charge equality, the valancies of anions must be equal to the sum of the valences (m + n) of cations. If the perovskites have the same valences as A and B, then all the ions in the system should have 8 electrons in their shells. If it has an odd value of A or B ions, then in their outer shells, [7] the ions in the structure may have more than 8 electrons. There are oxides of perovskite according to categories.

(1) If cations A and B belong to the first group and the elements of the 15^{th} group of the periodic table. Most of these compounds are either ferroelectric or antiferroelectric like $LiNbO_3$, $KNbO_3$, $AgNbO_3$, $AgTaO_3$ and $KTaO_3$ [8].

(2) If cation A belongs to elements of the second group and cation B belongs to elements of the periodic table of the fourth group. Some significant $A^{2+}B^{4+}O_3$

perovskite oxides are $CaTiO_3$, $SrTiO_3$, and $BaTiO_3$. These perovskite types can be used as dielectric and piezoelectric materials.

(3) Where both cations A and B belong to the third group of periodic table elements. Alkaline earth and trivalent ions (Y^{3+}, lanthanoids, Bi^{3+}, Tl^{3+}) on site A and tripositive transition metal ions on site B, i.e. oxides of type $A^{+3}B^{+3}O_3$ such as $BiFeO_3$, are present in this compound category. Such perovskites are used for functional materials because they have fascinating mixed conductivity properties of both ions and electrons or holes migration. A few systems display apparent oxygen defect, including $LaMnO_{3+\lambda}$, $Ba_{1-\lambda}La_{\lambda}TiO_{3+\lambda/2}$, $EuTiO_{3+\lambda}$ and $LaCuO_{3-\delta}$.

1.2. Perovskite substitution

It is possible to modify the ideal perovskite structure by doping two forms of B ions with suitable different size and charge. Ideal perovskites general formula is ABO_3, while $A_2BB'O_6$ or ($AB_{0.5}B'_{0.5}O_3$) is the general formula of perovskite after incorporation on B site. But the total charged on cations is equal to the oxygen ion charge. If the charge of B and B′ is different, with the ideal configuration of ABO_3 perovskite respectively, then the oxygen will be slightly moved towards the more charged cations and the symmetry of B and B′ cations will be retained. Substituted perovskite materials have a large number of technical uses, and their high dielectric constants (ε') and low tangent loss [9] are well stabilized. Both are technologically important materials even in un-doped form, as well as doping with various cations and modifying their properties [10, 11, 12, 13] Overall, there are two types of interstitial and substitution doping. Because perovskite is closely packed, it does not make an interstitial substitute. Perovskite has a great deal of versatility to replace A or B sites. It is therefore used by modifying their properties on the cation-site after replacement. Substitution modifications are affected by the following factors:

Oxides of perovskite can be replaced by the following types:

1.2.1. Isovalent substitution

1.2.2. Heterovalent substitution

1.2.3. Valence compensated substitution

1.2.1. Isovalent substitution:

The substituent ion and the ion it replaces have the same valence in isovalent substitutions. The ion it replaces on either A site or B site, or on both A and B sites simultaneously. For example, isovalent substitution, substitution of Ca, Sr or Pb at Ba at $CaTiO_3$ perovskite A site and substitution of Ti ion for isovalent substitution by Zr, Sn or Hf ions at B site.

1.2.2. Heterovalent substitution

It can be different valences on substitution in this substitution process. The replacement ion and the ion being replaced may also be on either A site or B site. To compensate for the extra charge, the resulting substituted perovskite will be produced. There are two types of heterovalent replacement.

(a) Acceptors substitutions:

When higher valencies were replaced by lower valancies at the solid compound site of A or B. the produces holes due to the production of oxygen vacancies and less contribution of electron from the substituent ion, e.g. Na^+ substitution on Ba^{2+} and Co^{3+} on the $BaTiO_3$ Ti^{4+} site [14].

(b) Donors substitutions:

A lower positive ion replaced on site A or B with a higher valence is known as donor replacement. In the crystal lattice of the host oxide, for example, La^{3+} or Y^{3+} on $Ba^{2+}$and Nb^{5+} on Ti^{4+} site in $BaTiO_3$ separately [15], the defect of the solid compound requires a species with an effective negative charge for charge compensation.

1.2.3. Valence compensated substitution:

There are two types of compensated substitution $M_{1-x}La_xTi_{1-x}M'_xO_3$ ($M_{1/4}$ Ca^{2+}, Sr^{2+}, Ba^{2+} or Pb^{2+} and $M'_{1/4}$ Co^{3+}, Ni^{3+}, Fe^{3+} etc) due to hetero valence and isovalent on A (e.g. $Pb_{1-x}Ba_xTi_{1-x}Sn_xO_3$) and B sub lattice site. When replacing a combination of ions at sub-lattice sites A and B [16, 17, 18], the crystal retains total electrical charge neutrality. In this case, on valence compensated solid solutions (VCSS), for example, there is a small chance of defect formation. La^{3+} ion simultaneously in $BaTiO_3$:$Ba_{1-x}La_xTi_{1-x}Co_xO_3$ on the Ba^{2+} site and Co^{3+} on Ti^{4+} site.

1.3. ABO_3 type high dielectric constant perovskites

A large number of perovskite type ABO_3 including $CaTiO_3$, $SrTiO_3$, $BaTiO_3$, etc. have a high dielectric constant.

1.3.1. Calcium titanate $CaTiO_3$

Mineral perovskite ($CaTiO_3$) is one of the few minerals with the distorted perovskite structure, although it has been suggested that the lower mantle of the Earth may consist mainly of $MgSiO_3$ perovskite [19]. Since $CaTiO_3$'s structural parameters derived from the [20] X-ray film analysis differs markedly from the systematic plots of other $GdFeO_3$-type perovskites [21], we refined its crystal structure. For this crystal [Koopmans, van de Velde&Gellings, (1983)], a powder neutron analysis has been published. $CaTiO_3$ has recently become aware of its biocompatibility and implant-bone applications [19, 20] in addition to its use in electronics [21]. In this respect, the actual mineral perovskite, $CaTiO_3$, is a good starting point because it is stable at room pressure and therefore suitable for different high temperatures measurements.

The $CaTiO_3$ class perovskites are typically characterized by a simple cubic lattice structure Drop-calorimetry measurements performed on $CaTiO_3$ perovskite between 400 and 1800 K showed the occurrence of two simultaneous phase transitions at 1384, and

1520 K. Calcium titanate has very little value except as one of the ores of titanium, along with several others. Titanium metal or ferrotitanium alloys are reduced to give metals.

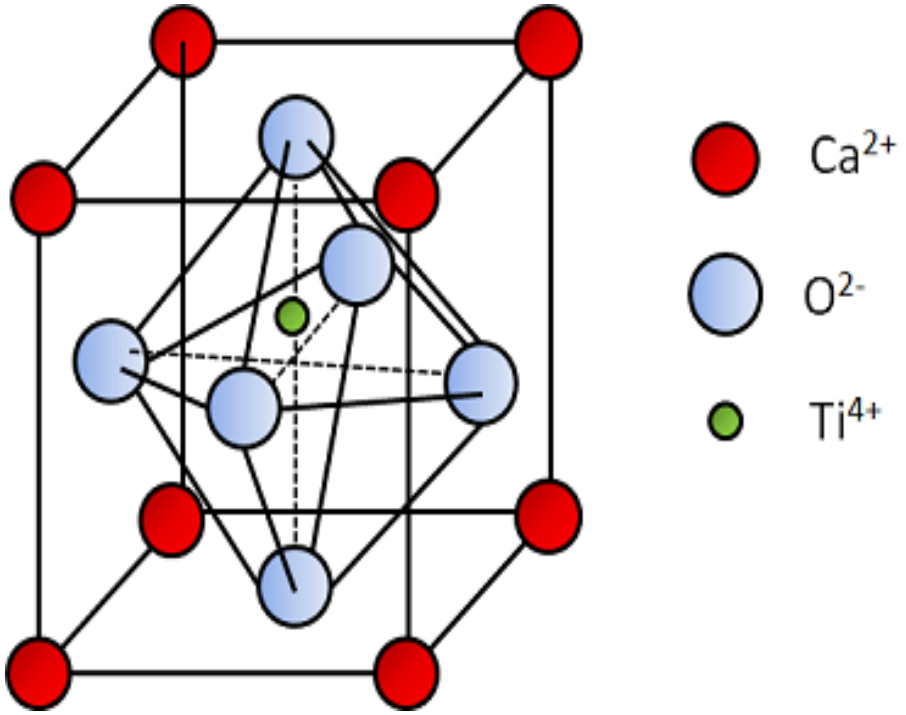

Figure 1.1. A perovskite unit cell that displays the titanium ion off-centered.

(a) Applications

Perovskite materials exhibit interesting and unusual physical properties that have been studied extensively for both practical applications and theoretical modeling, and perovskite materials science and applications have been a wide research area subject to many revolutionary discoveries for new device concepts. The potential applications of Perovskite are varied and include uses in sensors and catalyst electrodes, other types of fuel cells, solar cells, lasers, memory devices and applications for spintronics.

1.3.2. Barium Titanate ($BaTiO_3$)

Barium titanate ($BaTiO_3$ or BTO) has been synthesized as the first and most widely studied ceramic material because of its excellent dielectric, ferroelectric and piezoelectric properties [72]. $BaTiO_3$ ceramics high dielectric constant is the product of its crystal structure. As shown in Figure (1.2), $BaTiO_3$ has the perovskite structure. Each barium ion in Figure (1.2) is surrounded by 12 oxygen ions. A face-centered cubic lattice is formed by oxygen ions plus barium ions. The titanium atoms are surrounded by six oxygen ions in octahedral interstitial positions. The octahedral interstitial position in $BaTiO_3$ is quite large compared with the size of the Ti ions due to the large size of the Ba ions. The Ti ions in this octahedral position are too small to be stable. In the direction of each of the six oxygen ions surrounding the Ti ion, there are off-center minimum energy positions. The degree of polarization is very high because each Ti ion has a $^{4+}$ charge. The Ti ions can shift from random to aligned positions when an electrical field is applied, resulting in high bulk polarization and high dielectric constant [61]. There are three crystalline forms of barium titanate: cubic, tetragonal, and hexagonal. Due to its excellent ferroelectric, piezoelectric and thermoelectric properties, the tetragonal polymorph is the most widely used [73]. Temperature has a strong effect on the characteristics of $BaTiO_3$ crystal structure and polarization. $BaTiO_3$ is cubic above 120 °C (and up to 1400 °C) and the $BaTiO_3$ has, as described ab ove, a spontaneous random polarization. The Ti^{4+} ion is located in the center of an octae dron of oxygen ions in this temperature range (as shown in Figure 1.2. (a)).

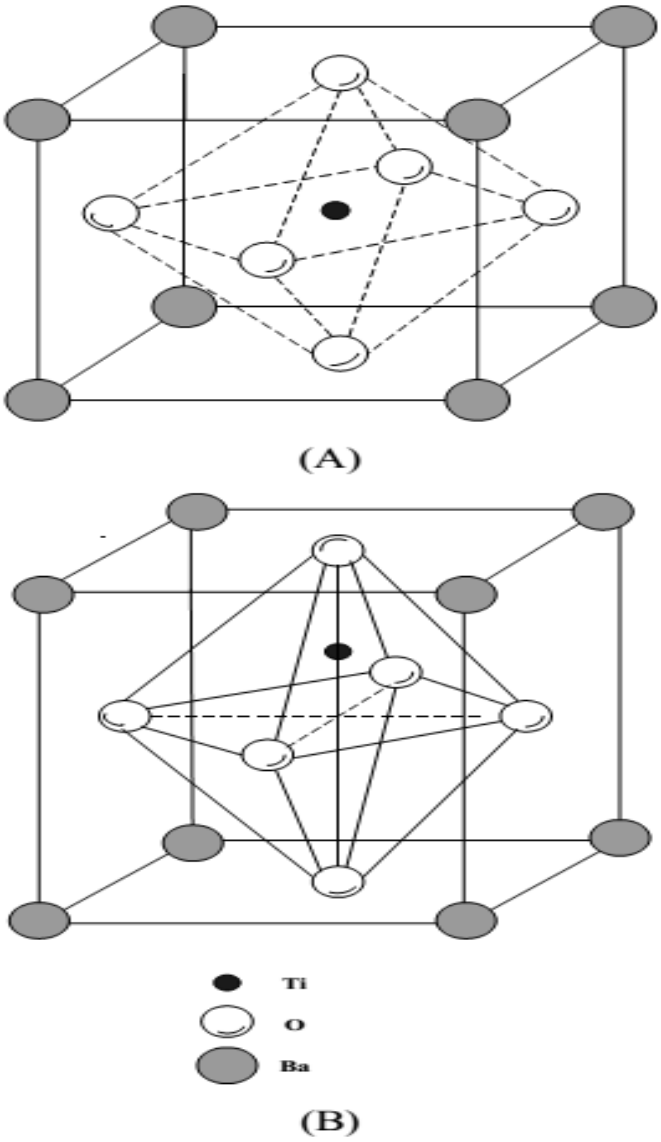

Figure 1.2. Schematic of the perovskite structure of $BaTiO_3$ (**A)** Cubic lattice (above Curie temperature, 120°C) (**B)** Tetragonal lattice (below Curie temperature, 120°C) [D. W. Richerson, 1992]

In its octahedral interstitial position in $BaTiO_3$, the thermal vibration is high enough to result in the random orientation of the titanium ions. The Ti^{4+} ion does change position, resulting in polarization when an electrical field is applied, but when the field is removed it returns to its stable central position. There is therefore no retained polarization, no loop of hysteresis, and no ferroelectric behavior. As $BaTiO_3$ temperature is slightly lowered below 120 °C (Curie temperature), there is a

displacement transformation in which the $BaTiO_3$ structure changes from cubic to tetragonal (Figure 1.2.(b)). The length of one crystallographic axis increases (unit cell from 4.010 to 4.022 Å) and the other two decrease in length (from 4.010 to 4.004 Å). The Ti^{4+} ion moves off-center towards one of the long axis ' two oxygen ions, leading to a spontaneous increase in positive charge in that direction. This is - 21 - shown in Figure 1.3. (a). Applying an electrical field opposite the polarity of this initial dipole would cause the Ti^{4+} ion to pass through the middle of the octahedral site and to travel to an identical off-centre. This can be seen in Figure 1.3. (b) Reversal polarization, hysteresis in the curve E versus P and ferroelectricity result. [61].

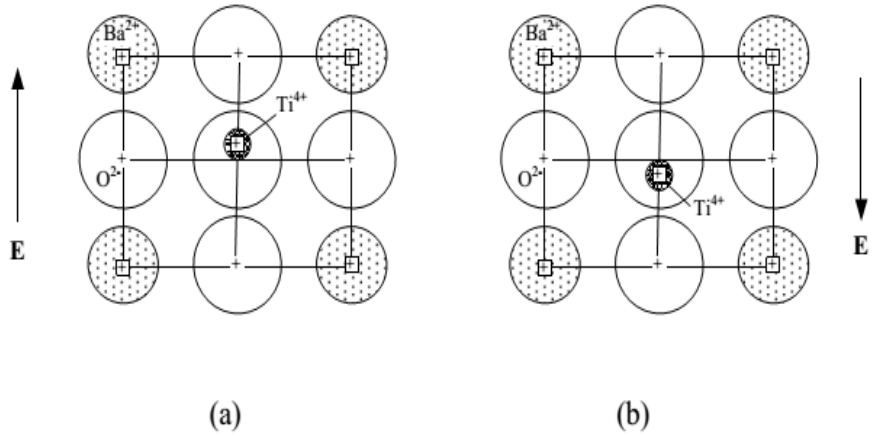

Figure 1.3. Reversal toward spontaneous polarization in $BaTiO_3$ by reversal of the applied field direction.

It was found that the dielectric properties of $BaTiO_3$ depend on the size and temperature of the grain. Because of the presence of multiple domains in a single grain, the motion of which walls increases the dielectric constant at Curie point, large-grained $BaTiO_3$ (around 10 μm) has a high dielectric constant at the Curie point.

For a fine-grained $BaTiO_3$ (~1 μm), there is a single domain within each grain. Grain boundaries restrict the movement of domain walls,

resulting in a low dielectric constant at the Curie point compared to coarse-grained $BaTiO_3$.

The dielectric constant of $BaTiO_3$ coarse-grained ceramics was found to be within the range of 1500-2000 at room temperature. On the other hand, fine-grained $BaTiO_3$ exhibits a room temperature dielectric constant between 3500-6000. This is because the internal stresses in fine-grained $BaTiO_3$ are greater than in the coarse-grained material, which leads to a higher permittivity at room temperature.

1.3.3. $SrTiO_3$

Such devices analysis and applications rely crucially on the knowledge of $SrTiO_3$ thin film properties. By applying a certain gate voltage, the $SrTiO_3$ layer dielectric constant determines the actual charge transferred to the superconductor. The charge that can be transferred to a device using $SrTiO_3$ as a dielectric layer is limited by the product $\varepsilon_{BD}E_{BD}$, where ε_{BD} is the dielectric constant ε evaluated at the breakdown field, E_{BD}. The findings for the dielectric behavior of bulk or single crystal $SrTiO_3$ [22, 23] have not yet been published for thin films. In this article, we present our findings in the actual structure of a high Tc FET system on the dielectric properties of thin $SrTiO_3$ films.

(a) Properties of strontium titanate

Table 1.1: Summary of the physical properties of $SrTiO_3$.

Property	Value
Lattice parameter at RT (nm)	0.3905
Atomic density (g/cm^3)	5.12
Melting point (°C)	2080
Mohs hardness	6
Dielectric constant (ε_0)	300
Thermal conductivity (W/m.K)	12
Coefficient of thermal expansion (Å/°C)	9.4×10^{-6}
Refractive index	2.31-2.38

(b) Crystal structure

In the ABO_3 cubic perovskite structure (space group Pm3 m), $SrTiO_3$ crystallizes at room temperature with a lattice parameter of 0.3905 nm and a density of 5.12 g/cm^3. Figure 2.1 sketches the crystal structure. The Ti^{4+} ions are coordinated six-fold by O2- ions, while four TiO6 octahedra surround each of the Sr^{2+} ions. Therefore, each Sr^{2+} ion is coordinated by 12 O^{2-} ions. While a hybridization of the O^{2-} p states with the Ti-3d states results in a pronounced covalent bonding [Leapman et al.(1982)] within the TiO_6 octahedra, Sr^{2+} and O^{2-} ions exhibit ionic bonding character. Therefore, $SrTiO_3$ has mixed bonding properties between ionic and covalent. This nature of chemical bonding results in a unique structure, making it an electronic material model.

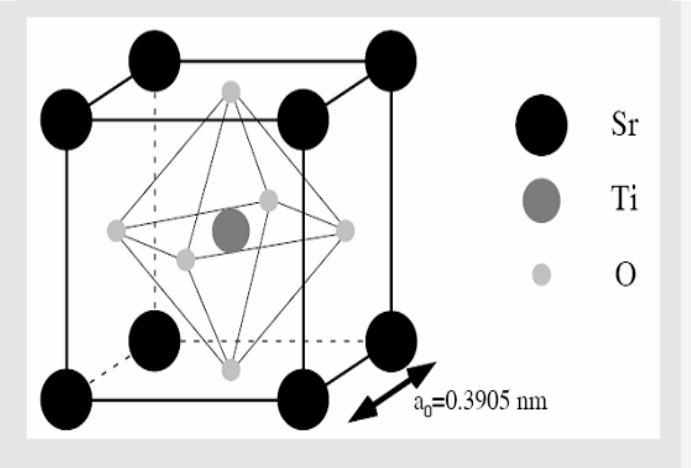

Figure 1.4. Atomic structure of $SrTiO_3$ at Room Temperature.

The sizes of the spheres representing the atoms are arbitrary and are not related to atomic radii. **Figure 1.4.** Shows some of the major (high-symmetry) axial direction atomic arrangements in $SrTiO_3$. There are always two distinct types of alternating equally spaced atomic planes with different is a real densities of the three constituent elements for any given planar direction (h, k, l) of a perovskite structure; in this case, Sr, Ti, and O. For example, there are two different types of atomic alternating planes on the (100) $SrTiO_3$ surface. One is generated by a plane of TiO_2 and the other by a plane of SrO [24].

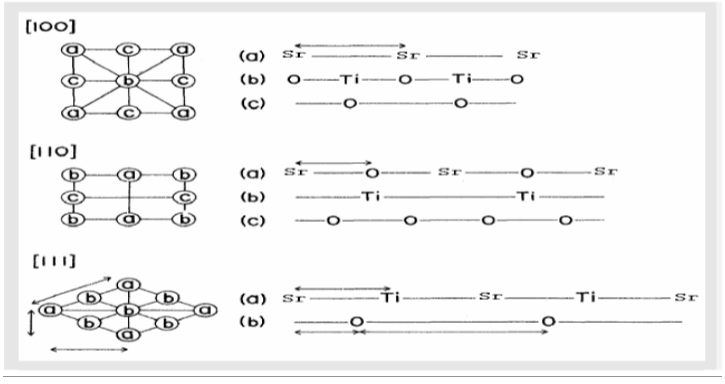

Figure 1.5. Atomic arrangements for the <100>, <110> and <111> axial direction in $SrTiO_3$.

The arrengements shown on the left are end views of the channels, and the letters refer to the individual rows shown on the right.

A distortion from cubic to lower symmetries occurs when the temperature is lowered or when a foreign cation / dopant (e.g. ion implantation) is inserted in the lattice. Three main effects are assigned to distortions: size effects, ideal composition deviations, and JahnTeller effect. Identifying a single effect as responsible for a certain perovskite's distortion is rare. Cubic $SrTiO_3$ at RT has three more phase transitions after cooling as an example of the complexity. $SrTiO_3$ bulk crystals are considered to be; tetragonal (a= b/c and Cmax= 0.39 nm; space group I4/*mcm*) between 110 K–65 K, due to the opposite rotation of the adjacent octahedra oxygen, orthorhombic in the range 55 K–35 K and possibly rhomboedral below 10 K as suggested by X-ray diffraction studies [25, 26]. There is actually no experimental evidence to confirm for sure which $SrTiO_3$ structure exhibits below 10 K. PAC studies on the subject have recently confirmed the existence of a single low-symmetry step at 10 K, which is not defined by axial symmetry [27].

1.4. Complex Peroskite

1.4.1. $CaCu_3Ti_4O_{12}$ (CCTO)

Calcium copper titanate (CCTO) has a chemical formula of approximately 100,000 for single crystal and 10,000 for bulk material at room temperature, $CaCu_3Ti_4O_{12}$, a novel electroceramics material with high dielectric permittivity (ε) and stability of phase transition against wide range temperatures (100–400 K). In (2000), Subramanian et al.[28] discovered that CCTO belongs to the $ACu_3Ti_4O_{12}$ family (A= Ca, Sr, Ba, $Bi_{2/3}$, $Y_{2/3}$, $La_{2/3}$) pseudo-cubic perovskite-related structure type oxide (space group: Im3) with a lattice parameter of 7.391 Å. The important value of e remaining constant over a wide range of temperatures from 100 to 400 K for CCTO makes its use in broad-ranging applications [29, 30, 31].

Engineering innovation requires a giant e-value material to reduce the size of electronic components, while efficient performance of these electronic components requires significantly low tan δ. For this reason, a significant number of theoretical and experimental researchers were conducted to reveal the existence and origin of the CCTO ceramics giant ε^r value. Various processing routes (chemical and physical methods) of CCTO were adopted such as solid-state reaction, wet chemistry route, sol–gel, solution combustion synthesis, sonochemical-assisted route, and co-precipitation [32, 33, 34, 35, 36]. $CaCu_3Ti_4O_{12}$ (CCTO) ceramics are potential candidates for capacitor applications due to their high dielectric permittivity (ε_r) values of up to 3×10^5. An internal barrier layer condenser (IBLC) system of insulating grain boundaries (GB) and conducting grain interiors (bulk) is the underlying mechanism for high ε'. This behavior is examined in detail, and discussed. The origin of the IBLC structure in nominally insulating $CaCu_3Ti_4O_{12}$ is due to a low Cu non-stoichiometry, which differs between the GBs and bulk.

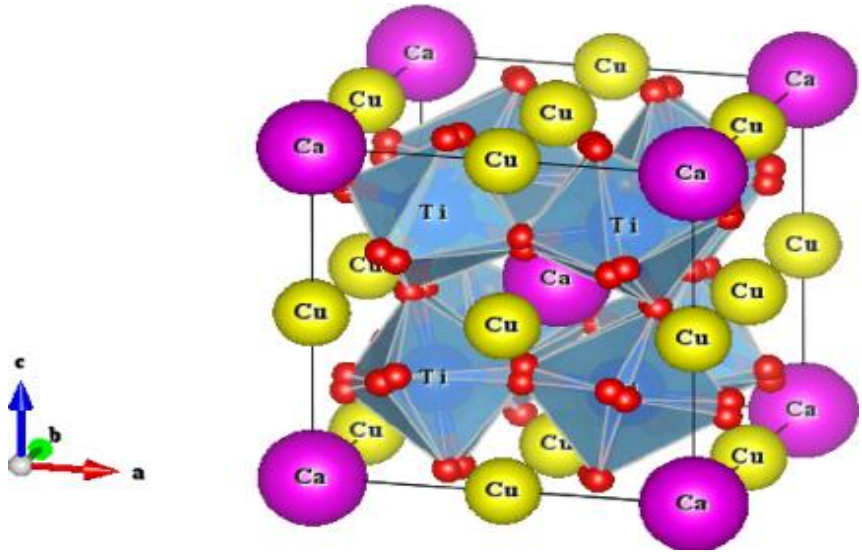

Figure 1.6. Crystal structure of CCTO compound.

These non-stoichiometric effects are analyzed in depth by examining bulk ceramics of different composition using X-ray diffraction (XRD), scanning electron microscopy (SEM) and impedance spectroscopy (IS) within the ternary CaO-CuO-TiO_2 phase diagram. There are proposed to be at least two fault mechanisms. It is further demonstrated that the development of the defect mechanisms in CCTO and the concomitant formation of the IBLC structure is strongly dependent on the processing conditions of CCTO ceramic pellets such as the sintering temperature. Using XRD, SEM, and Impedance Spectroscopy (IS), specifically stoichiometric CCTO bulk ceramics sintered at different temperatures are analyzed. There are proposed to be at least two fault mechanisms. It is further demonstrated that the production of the defect mechanisms in CCTO and the concomitant formation of the IBLC structure is strongly dependent on the processing conditions of CCTO ceramic pellets such as the sintering temperature. Using XRD, SEM, and Impedance Spectroscopy (IS), specifically stoichiometric CCTO bulk ceramics sintered at different temperatures are analyzed. CCTO ceramics output for IBLC applications is regulated by subtle modifications in the compound stoichiometry, which is strongly dependent on the temperature of the ceramic sintering.

1.4.2. $Y_{2/3}Cu_3Ti_4O_{12}$ (YCTO)

$Y_{2/3}Cu_3Ti_4O_{12}$ (YCTO) also represents an important class of ACTO series material. As mentioned in the literature [37, 38, 39] it is assumed to be isostructural to CCTO. It exhibits with excellent thermal stability with a high dielectrical constant. It too has the luxury of being lead-free and environmentally friendly. In our previous communications, at a relatively lower sintering temperature with substantial dielectric constant. We recorded the synthesis of YCTO ceramic by the semi-wet road.

The dielectrical properties were obtained through XRD, SEM, EDX and TEM analysis, as well as microstructural data.

The literature also reports the preparation of YCTO by the solid state reaction method [39] and sol gel process [41].

1.4.3. $Bi_{2/3}Cu_3Ti_4O_{12}$ (BCTO)

$Bi_{2/3}Cu_3Ti_4O_{12}$ (BCTO) is one of the few members that have been presently confirmed iso-structurally CCTO-like oxides. However, limited literature reported the BCTO ceramics prepared by the solid-state reaction [42, 43], and the dielectric constant of the ceramics is relatively low for practical applications. BCTO crystallizes as cubic perovskite-related structure as shown in Fig. 1 with space group Im3 and lattice constant a = 7.413 Å. [44, 45] In this structure, the Bi sites are 1/3 vacant to achieve charge-neutrality.

This could affect the dielectric behaviour, making this sample study more interesting.

The BCTO dielectric constant was started at 25 ^{o}C at 10^5 Hz to be 1870.

Although it is not as high as CCTO, it is still much broader than ordinary dielectrics.

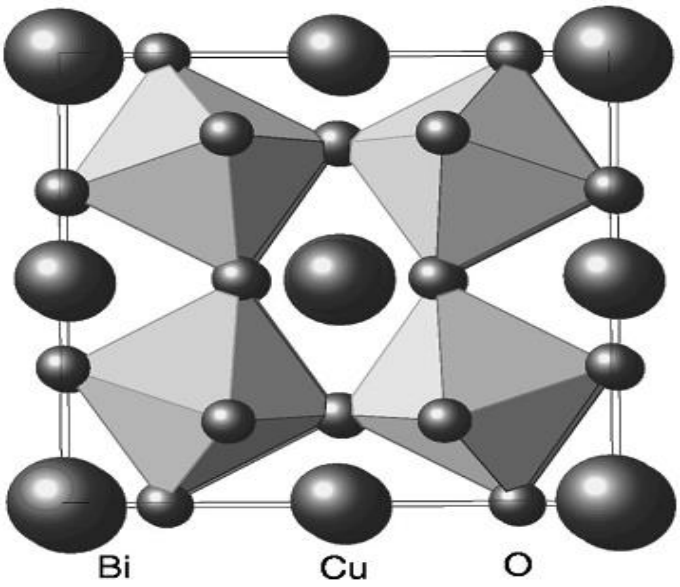

Figure 1.7. Crystal structure of BCTO, in which 1/3Bi sites are vacant. The Ti atoms sit at the center of the TiO_6 Octahedra.

1.6. Composite Introduction

The Composite material is a material made of two or more constituent materials with significantly different physical or chemical properties creating a substance with characteristics distinct from the individual components when combined. Inside the finished structure the individual components remain separate and distinct. For many purposes the new material may be preferred: common examples include materials that are stronger, lighter, or less costly than traditional materials. More recently, researchers have also begun to actively engage in composite sensing, actuation, computing, and communication [46].

1.6.1. Natural composites

There are natural composites in both the plants and animals. Wood is made of long cellulose fibers (a polymer) which a much weaker substance called lignin keeps together. Cellulose is present in cotton too, but it is much weaker without the lignin to tie it together. The two weak substances-lignin and cellulose-form a much stronger material together. The bone inside the body is a composite as well. It is made of a hard but brittle material called hydroxyl apatite (mostly calcium phosphate), and a thick, flexible material called collagen (which is a protein). Collagen is also present on fingernails and hair. It would not be much use in the skeleton on its own, but it can interact with hydroxyapatite to give bone the properties necessary to support the body.

1.6.2. Early composites

Several thousands of years ago, people made composites. An early example of that are mud bricks. Mud may be dried out to give a building material into a brick form. Its study if you try to crush it (it has decent compressive strength), but if you try to bend it

(it has can the tensile strength) it splits very quickly. Straw tends to be very powerful if you want to stretch it but you can quickly crumple it up. It is possible to make bricks that are resistant to both squeezing and tearing by mixing mud and straw, and make excellent building blocks. Concrete is yet another ancient composite. Concrete is a mix of aggregates, cement and sand (small stones or gravel).

It has a good compressive strength (resisting squashing), and in more recent times it has been found that adding metal rods or wires to the concrete can increase its tensile strength (bending). Reinforced concrete is called concrete containing such rods or wires.

1.6.3. Making composites

Many composites consist of only two components. One is either the matrix, or binder. It covers and links fibers or pieces of the other material, called the reinforcement, together. Modern examples Fiber glass was the first early composite material. Today it is still commonly used for boat hulls, sports equipment, construction panels and many car bodies. The matrix is a plastic, and the reinforcement is a glass made into fine threads and often woven into a kind of tissue. The glass on its own is very solid yet fragile, and if bent sharply, it will break.

The plastic matrix binds the fibers of glass together and also protects them from harm by exchanging the forces that act upon them. Many advanced composites are now manufactured instead of glass, using carbon fibers. These materials are lighter and stronger than fiber glass but more costly to manufacture. They are used in construction of aircraft and expensive sports equipment such as golf clubs. Carbon nanotubes were successfully used in the production of new composites too. These are even lighter and stronger than composites made from traditional carbon fibers, but they are still expensive. Nevertheless, they provide possibilities for producing smaller cars and

aircraft (which will use less fuel than the more huge vehicles we now have). The latest Airbus A380, the world's largest passenger airliner, uses modern composites in its construction. More than 20 per cent of the A380 consists of composite materials, primarily carbon fiber reinforced plastic. The proposal is the first large-scale use of glass-fiber-reinforced aluminum, a modern material that is 25 percent stronger but 20 percent lighter than traditional aluminum airframe.

1.6.4. Nanocomposite

It is a solid material with multiphase where one of the phases has one, two or three dimensions of less than 100 nanometers (nm) or structures with nanoscale repeat distanc es between the various phases that make up the material. the idea behind nanocomposite is to use nanometer-sized building blocks to design and create new materials with unprecedented flexibility and improvement in their physical properties. In the broadest sense, this definition may include porous media, colloids, gels, and copolymers, but is more commonly taken as the solid combination of a bulk matrix and nano dimensional phase. The nano composites mechanical, electrical, thermal, optical, electrochemical, catalytic properties may differ markedly from those of the component materials. Size limits for these effects were suggested [Kamigaito (1991)] < 5 nm for catalytic operation, < 20 nm for soft hard magnetic material, < 50 nm for refractive index changes and < 100 nm for super paramagnetism, mechanical reinforcement or restriction of the movement of matrix dislocation. Nano composite are found in nature, in the abalone shell and bone structure for example. The use of materials rich in nanoparticles long precedes the understanding of the physical and chemical nature of those materials. [47] investigated the origin of the color depth and acid resistance and bio corrosion of May a blue paint, attributing it to the mechanism of nanoparticles. Nano scale organo-clays have been used since the mid-1950s to control the flow of

polymer solutions (e.g., as paint viscosifiers) or the formulation of gels (e.g. as a thickening agent in cosmetics, holding the formulations homogeneous). By the 1970s the subject of textbooks was polymer / clay composites, [48] although the word Nanocomposite was not widely used. In mechanical terms, because of the exceptionally high surface-to-volume ratio of the reinforcing process or its abnormally high aspect ratio, nano composites vary from traditional composite materials.

The material for reinforcement may consist of particles (e.g. minerals), sheets (e.g. exfoliated clay stacks) or fibers (e.g. carbon nanotubes or electrospunfibres). The interface region between the phase of matrix and reinforcement is usually an order of magnitude greater than that for standard composite materials. The matrix material properties in the vicinity of the reinforcement are significantly impacted. [Ajayan et al] note that with polymer nano composites, local chemistry related features, degree of polymer chain ordering or crystallinity can all vary significantly and continuously from the reinforcement interface to the bulk of the matrix. A large amount of strengthening surface area means that a relatively small amount of nanoscale reinforcement can have an observable effect on the composite's macro scale properties. The addition of carbon nanotubes for example improves the electrical and thermal conductivity. Certain forms of nanoparticles can result in enhanced optical properties, dielectrical properties, heat resistance, or mechanical properties such as rigidity, strength, and wear and damage resistance. In general, during processing the nano-reinforcement is dispersed into the matrix. The percentage by weight (called mass fraction) of the nano particulates introduced can remain very low (on the order of 0.5% to 5%) due to the low filler percolation threshold, especially for the most commonly used non-spherical, high aspect ratio fillers (e.g. nanometer-thin platelets, such as clays, or nanometer-diameter cylinders, such as carbon nanotubes).

The orientation and arrangement of asymmetric nanoparticles, thermal property mismatch at the interface, interface density per unit volume of the nano composite, and poly dispersity of nanoparticles significantly affect the effective thermal conductivity of nano composites.

1.6.5. Ceramic matrics nano composite

The main part of the volume in this group of composites is filled by a ceramic, i.e., a chemical compound from the group of oxides, nitrides, borides, silica, etc. In most cases, nano composites for the ceramic-matrix include a metal as the second component. Ideally, all elements, the metallic component and the ceramic component, are finely scattered to evoke the specific nano scopic properties within each other. To improving their optical, electrical and magnetic properties [49] as well as tribological, corrosion-resistant and other protective properties [50], nano composite from these combinations has been demonstrated. When developing ceramic-metal nano composites, the binary phase diagram of the mixture should be considered, and measures must be taken to prevent a chemical reaction between both components. The last point is of primary importance for the metallic component which can react easily with the ceramic and thus lose its metallic character. This is not an easily obeyed limitation, because the ceramic part preparation requires high process temperatures. Therefore, the best approach is to carefully select the immiscible metal and ceramic phases. The ceramic-metal composite of TiO_2 and Cu, the mixtures of which were found to be immiscible over large areas in the Gibbs triangle of Cu-O-Ti [Effenberget al. (2001)], is a good example for such combination. The principle of ceramic-matrix nano composites has also been extended to thin films which are solid layers of a few nm to some tens of μm thickness deposited on an underlying substratum and which play an important role in the functionalization of technological surfaces. As a potentially useful technique for the preparation of nano

composite structures, gas flow sputtering through the hollow cathode technique turned out. The process operates as a technique of vacuum-based deposition and is associated with high rates of deposition up to some μm/s and growth of nanoparticles in the gas phase. Nanocomposite layers in the composition range of ceramics were prepared from TiO_2 and Cu using a hollow cathode technique [51] which showed high mechanical strength, low friction coefficients and high corrosion resistance.

1.6.6. Application of composites

Modern composite materials most prominent advantage is that they are both light and durable. Through choosing a suitable combination of matrix and reinforcement material, a new material can be created that meets exactly the specifications of a particular application. Composites also provide flexibility in design, since many can be molded into complex shapes. Often the downside is the cost. The resulting product is more efficient, but the raw materials are often costly.

1.7. Ceramic Dielectrics

Dielectrics are those isolators that do not flow charges, but shift from their average position of equilibrium, causing polarization. When a dielectric material is put in an electric field, a dimensionless quantity called the dielectric constant defines the amount of polarization induced. A typical dielectric example is the electrically insulating material between the metallic plates of a condenser. The dielectric polarization by the applied electric field raises the surface charge of the condenser for the given intensity of the electric field. The following sections will describe dielectric constant, dielectric resistivity, dielectric loss and dielectric force:

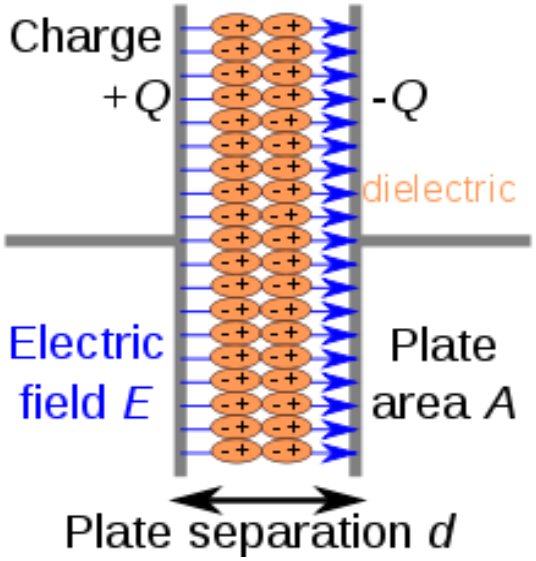

Figure 1.8. A polarized dielectric material.

1.7.1. Dielectric Behavior

(a) Basic knowledge on dielectric capacitor

A condenser consists of two plates packed with certain dielectric materials. As shown in Figure 1.8, it is popular in the parallel-plate shape. Dielectric materials are role of condenser bases in electronics devices. Capacitors have an energy-storage capacity that is determined by dielectric permittivity and conductor geometry. This phenomenon is known as C denoted capacitance. The potential difference between the conductors and the overall charge on them is independent. The dielectrics are held between two parallel plates, and capacitance is roughly the same as:

$$C = \varepsilon' \varepsilon_0 \frac{A}{d} \qquad (1.2)$$

Where C is the capacitance, where C is the relative permittivity, ε_0 is the electrical constant ($\approx 8.85\times10^{-12}$ Fm-1), A is the overlapping area of the two plates, and d is the distance between the plates. Clearly, the capacitance is inversely proportional to the amount of separation between the plates, while being directly proportional to the thickness of the plates of the conductor and the relative permittivity of the dielectrics.

The electric polarization happens when an external voltage V is applied on the plates of the conductor. The positive and negative pressures will accumulate with equal weight on the two plates. It is called capacitor charging phase. The electrical potential (caused on both plates by the cumulative charge ± Q) is equal to the externally applied voltage V, and then the charging cycle is completed. Q/V is equivalent to condenser capacitance C. Often, the external bias affects the relative permittivity of the dielectrics, allowing the capacitance to differ. In this case, capacitance relating to incremental change is defined:

$$C = \frac{dq}{dv} \qquad (1.3)$$

During the charging process, the charges are shifted by the role of external bias between the conductor plates, meaning that work has to be done and that the electrical energy is simultaneously retained in the dielectrics. Consequently, the amount of energy accumulated by W could be derived from the formula:

$$W = \int_0^Q V dq = \int_0^Q \frac{q}{C}\, dq = \frac{1}{2}\frac{Q^2}{C} = \frac{1}{2}\, CV^2 = \frac{1}{2}VQ. \qquad (1.4)$$

The detailed dielectrical properties in perovskite were studied after the discovery of ABO_3 perovskites such as $BaTiO_3$ and $PbTiO_3$ [52]. The high dielectric constant in microelectronics is required for capacitive parts. The high dielectric constant of perovskite is dependent on the oxygen lattice polarization of the metal ions. Examples of disordered solid solutions such as (1-x)$PbZn_{1/3}Nb_{2/3}O_3$.x$PbTiO_3$ (PZN-PT) [53] and (1-x)$PbMg_{1/3}Nb_{2/3}O_3$.x$PbTiO_3$ (PMN-PT) are relaxor ferroelectrics with a high dielectric constant. A change of the dielectric constant is also expressed as a result of temperature and dispersion of frequencies with great dielectric constants. Giant dielectric constant materials have found extreme importance in applications such as metal-oxide semiconducting field effect transistors (MOSFET's) for capacitor,

microelectronics, and microwave devices and equipment implementation. The ceramics $CaCu_3Ti_4O_{12}$ display a giant dielectric constant of about 10^4, which is almost constant from room temperature to 573 K [45, 54, 55, 56]. One of the main reasons for the origin of high dielectric constant is the barrier layer condenser model; it has been stated in the literature. The compound Li-ion conductor $La_{0.67}Li_{0.25}Ti_{0.75}Al_{0.25}O_3$ is known as a dielectric material with high electrical resistivity [37] but as an effective electrostatic field supporter.

The energy can be retained by an electrostatic field when there is no interference of the electrostatic flux lines and minimal current between opposite electric poles. This phenomenon can find applications in virtually any electricity-driven system, and is useful in [57] capacitors. Different condenser forms are based on dielectric materials with perovskite structure from BaTiO3, $PbMg_{1/3}Nb_{2/3}O_{3x}$ [PMN], $PbZn_{1/3}Nb_{2/3}O_{3x}$ [PZN], and $Pb_{1-x}La_x(Zr_{1-y}Ti_y)O_3$ [PLZT]. [58] $BaTiO_3$, $CaTiO_3$ and $SrTiO_3$ Ceramics are used as energy storage materials. Recently, [59] are using the manufacture of superior dielectrics in Wireless telecommunication. Dielectrics are primarily insulators which can be polarized by electric field application. When a dielectric material is put in an electric field, electrical charges do not flow through it (as in conductors) but change from their average position of equilibrium, causing polarization. The amount of polarization caused is described by a dimensionless quantity called the dielectric constant.

1.8. Polarization

By putting in an electric field, the positive and negative charges of dielectrics are displaced throughout the dielectric volume by very small distances from their equilibrium positions. These results in a large number of dipoles being produced each having a certain dipole moment in the direction of the field. It is said that the substance

is polarized by a polarization P. The polarization is known as the dipole moment per unit volume.

1.8.1. Types of polarization:

(a) Electronic polarization:

This kind of polarization occurs in the presence of an applied electric field, leading to the displacement of an atoms electron cloud compared to its nucleus. The polarization, as well as the material's dielectric constant at optical wavelengths, comes mainly from electronic polarization. This mechanism will result in low dielectric constant, up to 2–4, and can respond to very high frequencies about 10^{15} Hz.

(b) Ionic polarization:

Ionic polarization occurs from the movement of a charged ion in a solid relative to other ions. The ionic contribution at low frequencies is significant.

(c) Dipolar polarization

Molecular (dipolar) polarization occurs due to polar substances that, in the presence of an external electric field, may orient themselves. The molecules thermal agitation appears to counteract the ordering effect of the electric field, and a state of equilibrium is reached whereby the various dipoles make all possible angles ranging from zero to π radians with the direction of the field. This occurs at about 10^{11} to 10^{12} Hz.

(d) Space charge polarization:

Space charge (interfacial) polarization arises due to the accumulation of charges at the surface of a polycrystalline material or the grain boundaries. In response to the field-giving rise applied, the ions disperse across appreciable distances to re-distribution of charges in the dielectric medium [60]. The standard frequency range for this polarization is about 10^{-3} to 10^{3} Hz.

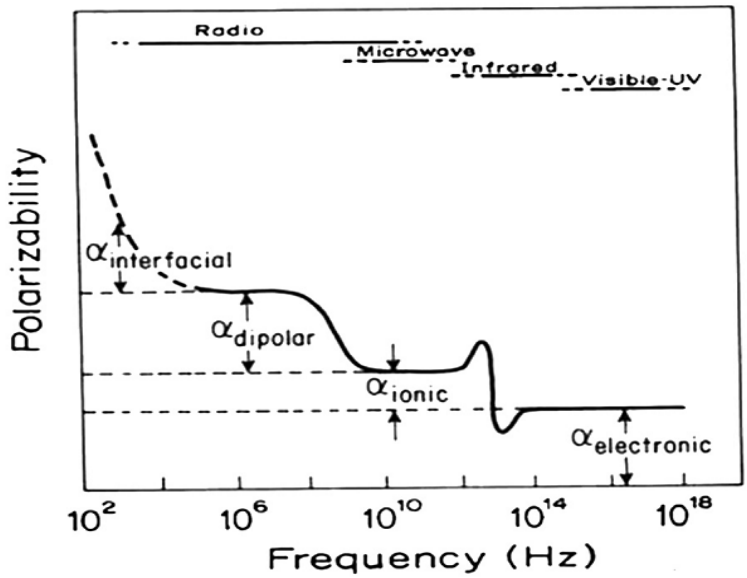

Figure1.9. Typical response of the total polarizability of a crystal as a function of electric field Frequency.

$$P = P_{electronic} + P_{ionic} + P_{molecular} + P_{interfacial}$$

(1.5)

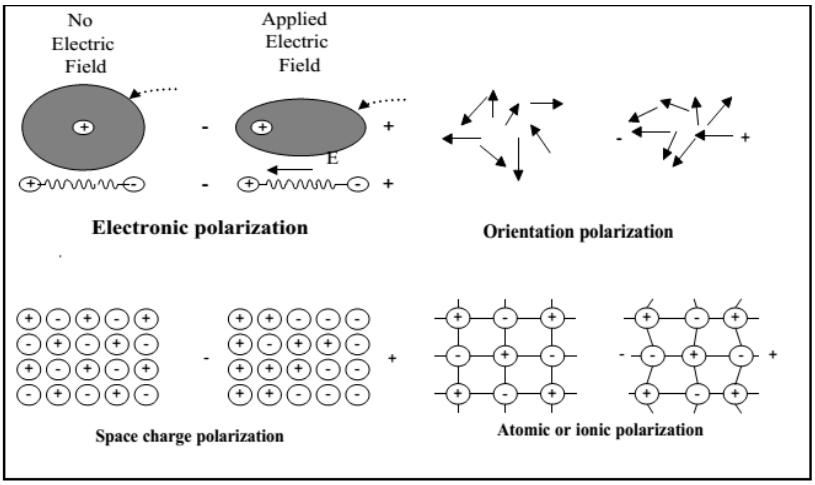

Figure 1.10. Types of polarization mechanisms [61, 62].

1.9. Dielectric constant

The dielectric constant is the ratio of a substance's permittivity to the allow ability of free space. It is an expression of how much electrical flux a substance concentrates, and is the electrical equivalent of relative magnetic permeability. Dielectric constant is the element by which the efficiency of a parallel-plate condenser is increased by adding a dielectric instead of a vacuum. Insulator materials with low conductivity of approximately 20 orders of magnitude are the product of energy band gaps of more than 2 eV (compared to zero for metals). Such dielectric materials constitute an essential part of the electronics market. The dielectric constant is a physical quantity that has the ability of material to polarize in response to the field. It reduces the total electric field inside the material [63, 64].

1.10. Dielectric loss

Dielectric loss quantifies the intrinsic dissipation of electromagnetic energy (e.g., heat) from a dielectrical material. It can be parameterized either in terms of the angle of loss (tan δ) or the corresponding tangent of loss tangent (tan δ). These apply to the phase or in the complex plane, the real and imaginary parts of which are the resistive (lossy) portion of an electromagnetic field and its reactive (loss less) counterpart. Dielectric loss, tangent loss that heats a dielectric material in a varying electric field. For example, each half cycle is charged and discharged alternately by a capacitor incorporated in an alternating-current circuit. During the alternation of the plate’s polarity, the charges must be displaced through the dielectric first in one direction and then in the other, and overcoming the resistance they experience leads to the creation of heat by dielectric loss, a function that must be considered when adding capacitors to electrical circuits, such as those in radio and television receivers. Dielectric losses depend on the dielectric material and the frequency. Heating by dielectric loss is commonly used industrially to

heat thermosetting glues, to dry foam rubber and other fibrous materials, to pre heat plastics before molding, and to rapidly jell and dry foam rubber. The dielectric loss (tan δ) is a material property and a measure of energy loss in the dielectric during cooperation. It does not depend on the geometry of capacitor. The dielectric loss is expressed as the loss tangent (tan δ) or dissipation factor can be defined as equation (1.6).

$$\tan\delta = \frac{\varepsilon''}{\varepsilon'} + \frac{\sigma}{2\Pi f \varepsilon'} \qquad (1.6)$$

Where ε′ is the real part, and ε″ is the imaginary part of the dielectric permittivity, and σ is the electrical conductivity of the materials and f is the frequency. Dielectric loss (tan δ) results from lack of distortion, dipolarity, interfacial loss, and conductivity. The loss of distortion is attributed to processes of electronic and ionic polarization and at area of high frequency. The interfacial failure stems from the highly polarized interface the fillers induce. The main cause of dielectric failure in dielectric materials is the rotation of atoms or molecules in an alternating electric field. The conduction loss represented the flow of actual charge through the dielectric materials and attributed to the dc electrical conductivity of the materials. The dielectric constant is usefulness of dielectric as an insulator material which is given by equation (6).

$$\varepsilon'' = \frac{\tan\delta}{\varepsilon'} \qquad (1.7)$$

Where ε′ is dielectric constant and tan δ is the dielectric loss of dielectric materials. For this purpose, it is desirable to have a low dielectric constant and particularly a minimal loss angle. The energy loss in dielectric materials results from three processes as follows:

i) Ionic migration losses (i.e., DC conductivity)

ii) Relaxation losses for dipole reorientation due to ionic jump and

iii) Ion vibration and deformation losses.

iv) The energy loss (W) is proportional to the dielectric loss tangent (tan δ) and refers to the energy dissipated in a dielectric material. This can be determined by the following equation:

v) $W = \Pi\varepsilon'\xi^2 f tan\delta$ (1.8)

Where ξ is the electric field strength and f is the frequency. Hence, a low dielectric loss is preferred to reduce the dissipation of energy and particularly for high frequency applications. A dielectric loss below 5 % is generally considered high, and 0.1 per cent is pretty low. Applications for radio frequency (RF) often rely on low loss tangent due to avoiding signal losses but much higher values can be tolerated for applications for energy storage, such as decoupling. In the high-temperature area, the presence of oxygen vacancies is an imperative, and free carrier conductivity causes a rapid increase in the dissipation factor. The doping and temperature depend on the concentration of free carriers. The dissipation factor (tan δ) in high-temperature range is inversely proportional to the frequency.

Polycrystalline titanates on cooling, rapid re-oxidation occurs above 1100 °C but essentially stops between 600 °C and 900 °C at some temperatures. The outside of each grain is therefore well oxidized while the inside of the grains remains deficient in oxygen. The oxygen vacancies on the titanium atoms were neutralized by 3d electrons and produced two Ti^{3+} ions for each oxygen vacancy. Ti^{3+} ions and vacancies in oxygen are bound by a low energy of 0.10–0.20 eV. Ti^{3+} equipped with conductive electrons, using the narrow 3d conductive band. The dissipation factor (tan δ) in high-temperature range is inversely proportional to the frequency. Polycrystalline titanates on cooling, rapid re-oxidation occurs above 1100 °C but essentially stops between 600 °C and 900 °C at some temperatures. The outside of each grain is therefore well oxidized while the

inside of the grains remains deficient in oxygen. The oxygen vacancies on the titanium atoms were neutralized by 3d electrons and produced two Ti^{3+} ions for each oxygen vacancy. Ti^{3+} ions and vacancies in oxygen are bound by a low energy of 0.10–0.20 eV. Ti^{3+} equipped with conductive electrons, using the narrow 3d conductive band. As a consequence, the conduction process can be described as electron hopping as following equation (1.9).

$$Ti^{3+} \leftrightarrow Ti^{4+} + e^{-} \qquad (1.9)$$

And unattached oxygen vacancies also contribute to the conductivity, but their mobility is much smaller than that of electrons [65]. The knowledge of a torque that appears to match the moment of the dipole moment of the applied force, and neutralized bound defects are not directly involved in the conduction process. In that process, the dielectric polarization and dielectric loss are formed.

1.11. Basic Principles of Impedance Spectroscopy

Temperature-dependent impedance spectroscopy (IS) helps to deconvoluted and classifies separately various contributions to the dielectric and resistive properties of condensed matter [66, 67]. Impedance Spectroscopy (IS) is therefore the method of choice to assess and investigate separately the dielectric properties of GB and grain indoor (bulk) regions in electrically inhomogeneous electroceramics such as CCTO [68]. It is well known that specific dielectric relaxation processes have been observed by IS such as those found in GB and bulk regions. In the simplest case, the brickwork layer model should be understood in which each GB or bulk form contribution is represented by one RC circuit part consisting of a parallel resistor and condenser [69]. Several dielectric relaxations in series can be characterized by several RC elements connected in series, where the macroscopic impedance is only the sum of all RC impedances in series. The RC model works especially well for insulators such as dielectrics, where the

condenser explains the material's ability to store energy, and the parallel resistor shows the current of leakage due to some un-trapped load carriers by passing the ideal storage item.

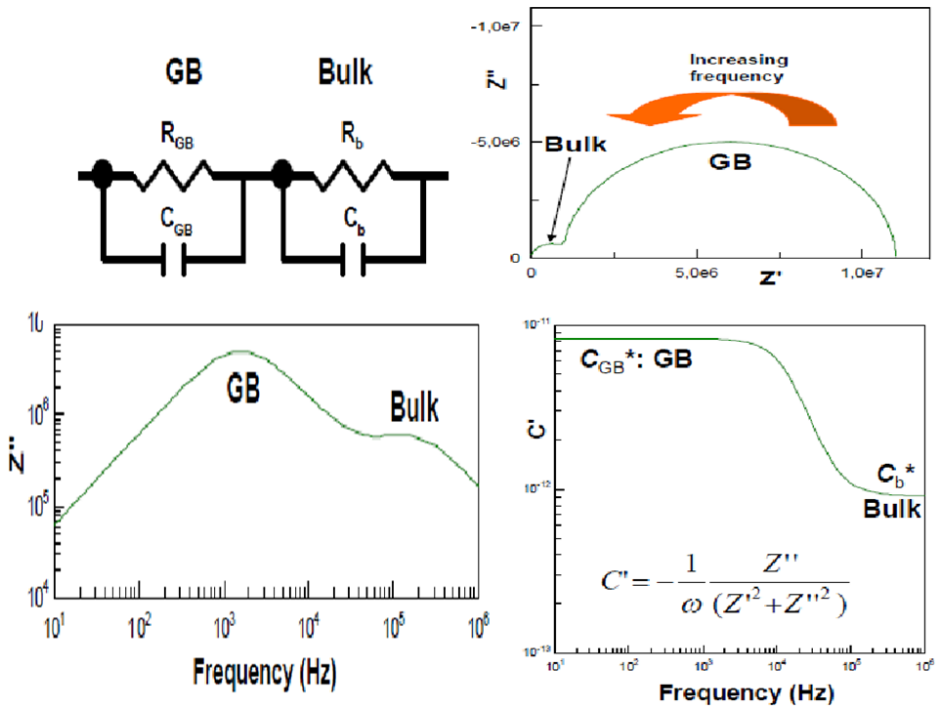

Figure 1.11. Simulated IS data for two RC elements connected in series, presented in different formats: Z" [Ω] vs. frequency (f), M" vs. f, Z" [Ω] vs. Z' [Ω] and C' [Farad] vs. f. Simulations were carried out with RGB = 10 MΩ, Rb = 1 MΩ, CGB = 10 pF and Cb = 1 pF.

Impedance Spectroscopy data can also be represented in alternative formats using the standard conversions shown in **Figure 1.11.** For the real part of the dielectric permittivity (ε') or capacitance (C′). Such plots often contain important information on the resistance or permittivity of a specific relaxation. In a scenario of a ceramic sample such as CCTO with one GB and one bulk (b) relaxation as represented by two RC elements connected in series, the following spectral features are expected as shown from the simulations presented in **Figure 1.11**.

(a) In plots of Z′ vs. Z″ two semicircles appear with each semicircle diameter corresponding to the respective resistance *R*,

(b) *Z*'' vs. frequency (*f*) plots show two relaxation peaks with peak heights of *R*/2 for each relaxation,

(c) *C*' vs. *f* or ε' vs. *f* display two approximately *f* independent *C*' (ε') plateaus C_{GB}^* and C_b^*, thatcorresponds approximately to the GB (C_{GB}) and bulk capacitance (C_b) and show an average sharp drop at a distinct *f*.

The resistance and capacitance values were chosen to represent a realistic scenario of one extrinsic GB- and one intrinsic bulk-type relaxation. In the framework of the brickwork layer model of two RC elements connected in series, the GB and bulk capacitance plateau C_{GB}^* and C_b^* depicted in the *C*′ vs. *f* plot in **Figure 1.11** are both only an approximation for the G_b and bulk capacitance C_{GB} and C_b respectively. Where C_{GB}^* contains all resistor and capacitor terms and C_b^* contains a contribution from the GB capacitance. The C_{GB}^* and C_b^* do not coincide exactly with the values of the capacitors C_{GB} (10 pF) and C_b (1 pF). The exact expressions for C_{GB}^* and $C_b^*$are given by equations (1.10) and (1.11) respectively.

$$C_{GB}^* = \frac{R_{GB}^2 C_{GB} + R_b^2 C_b}{(R_{GB} + R_b)^2} \qquad (1.10)$$

$$C_b^* = \frac{C_{GB} \times C_b}{C_{GB} + C_b} \qquad (1.11)$$

The GB and bulk resistance R_{GB} and R_b are sufficiently different, i.e. R_{GB} » R_b, then C_{GB}^* constitutesan excellent estimate for C_{GB}. This is usually the case for CCTO where R_{GB} and R_b commonly vary by more than 3 orders of magnitude. C_b^* is a good estimate for C_b for the case where the two capacitors C_{GB} and C_b are sufficiently different, i.e., C_{GB} » C_b. *Z*'' vs. *f* plots highlight the relaxation peak with the highest resistance *R* (e.g. the GB peak in CCTO).The approximate peak frequencies for GB or bulk relaxation peaks as

depicted in **Figure 1.11** are given in equation 4 for the respective plots of -*Z*'' vs. *f* (GB) using two ideal RC elements connected in series. Equation (4) implies an extrinsic GB-type relaxation with large resistance and capacitance to appearat lower *f* than the bulk, which is a common feature in experimental impedance spectra from electroceramics.

1.12. Conductivity

The degree to which a specified material conducts electricity, measured as the ratio of the materials current density to the electrical field that induces the current flow. The rate at which heat moves through specified materials, expressed as the amount of heat that flows per unit time through a unit area with a temperature gradient of one degree per unit.

1.13. Magnetic Properties

Ceramic's magnetic properties are the significant class of materials that have a variety of applications including data storage, tunnel junction, and spin valves. The magnetic ceramic materials have certain unique properties such as magnetic coupling, low loss and high electrical resistivity which have been altered by material structure and composition [70]. A system's magnetic moment tests the magnetism's power and direction. Typically the term itself refers to the moment of the magnetic dipole. Anything that is magnetic has a magnetic moment, like a bar magnet or a loop of electric current. A magnetic moment is a quantity of waves, with a direction and magnitude. The electron has a magnetic electron dipole moment, created by the intrinsic spin property of the electron, which gives it an electric charge in motion. Including paramagnetism, diamagnetism, ferromagnetism, antiferromagnetic and ferromagnetic, there are many different magnetic behaviors.

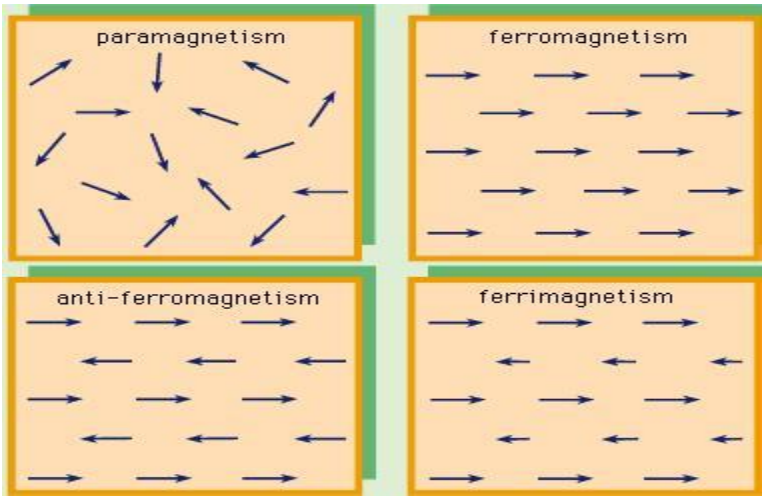

Figure 1.12. Types of Magnetism.

The ability to form magnets is an important feature of transition metals. Metal complexes are magnetic, with unpaired electrons. This magnetism must be due to having unpaired d electrons, since the last electrons live in the d orbitals. The spin of a single electron is denoted as + (1/2) or - (1/2) by the quantum number m_s. If the electron is coupled with another, this spin is negated, which produces a weak magnetic field when the electron is unpaired. Further unpaired electrons boost the effects of paramagnetic action.

The electron configuration of a transition metal (d-block) changes in a coordination compound; this is due to the repulsive forces between electrons in the ligands and electrons in the compound. Depending on the strength of the ligand, the compound may be paramagnetic or diamagnetic.

1.13.1. Magnetism

At its root, arises from two sources:

(a) Electron magnetic moment

The electron magnetic moment is an electron's magnetic moment caused by its inherent spin and electric charge properties.

The magnetic moment value of the electron is about -9284.764×10^{-27} J/T. Recently the electron magnetic moment was calculated at a precision of 7.6 parts in 10^{13} [71]. The electron is a charged charging particle, −1e, where e is the elementary charge unit. The angular momentum originates from two rotational types: spin and orbital motion. A revolving electrically charged body from the classical electrodynamics produces a magnetic dipole with magnetic poles of equal magnitude but opposite polarity. This analogy holds that an electron actually acts as a tiny bar magnet.

One consequence of that is that an external magnetic field exerts a torque on the magnetic moment of the electron depending on its field orientation.

(b) Spin magnetic moments

Usually, the magnetic moments of the nuclei of atoms are thousands of times smaller than the magnetic moments of the electrons; therefore they are negligible in the sense of material magnetization. Nonetheless, nuclear magnetic moments are very important in other contexts, especially in nuclear magnetic resonance imaging (NMR) and magnetic resonance imaging (MRI). The enormous number of electrons in a substance is normally organized in such a way that their magnetic moments (both orbital and intrinsic) cancel out. This is due to the combination of electrons in pairs with opposite intrinsic magnetic moments as a result of the Pauli Exclusion Principle, or in combination with zero net orbital motion into filled sub-shells. In both cases, the arrangement for electron is precisely to cancel the magnetic moments from each electron. However, even if the electron structure is such that unpaired electrons or unfilled sub-shells are present, it is often the case that the various electrons in the solid contribute magnetic moments pointing in separate, random directions so that the substance is not magnetic. Often, either naturally or due to an external magnetic field

applied, each of the magnetic electron moments will be lined up on average. Instead, an effective material may produce a strong net magnetic field.

For the reasons mentioned above, the magnetic behavior of a material depends on its structure, particularly its electron configuration, and also on the temperature. At high temperatures spontaneous thermal motion makes preserving equilibrium more difficult for the electrons.

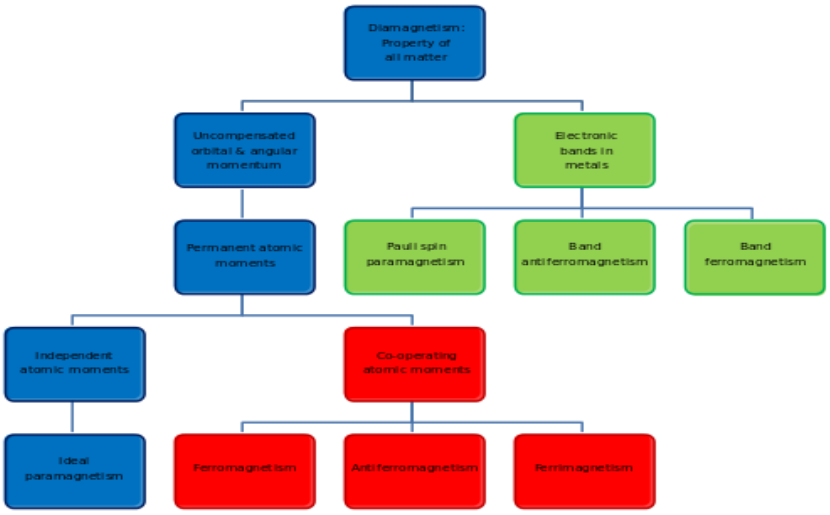

Figure 1.13. Flow chart of Magnetism.

1.13.2. Diamagnetic

Diamagnetism appears in all materials and is the tendency of the material to oppose an applied magnetic field, and therefore, to be repelled by a magnetic field. However, in an article with paramagnetic properties (that is, with a tendency to enhance an external magnetic field), the paramagnetic behavior dominates. Thus, despite its universal occurrence, the diamagnetic response is observed only in a purely diamagnetic material.

In a diamagnetic material, there are no unpaired electrons, so the intrinsic electron magnetic moments cannot produce any bulk effect.

In these cases, the magnetization arises from the electrons orbital motions, which can be understood classically as follows:

When a substance is put in a magnetic field, the electrons that surround the nucleus will undergo a Lorentz force from the magnetic field, in addition to their Coulomb attraction to the nucleus. This force may increase the centripetal force on the electrons, pulling them in toward the nucleus, or decrease the force, pulling them away from the nucleus, depending on which direction the electron is orbiting. This effect systematically increases the magnetic orbital moments aligned opposite the field and decreases those aligned parallel to the field (by the law of Lenz). It results in a small magnetic moment in bulk, with a direction opposite to that applied. Remember that this explanation is intended only as heuristic; a proper understanding includes a description of the quantum-mechanical existence. Note that this orbital response is subjected to all materials. However, the diamagnetic effect is overwhelmed by the much stronger effects caused by the unpaired electrons in paramagnetic and ferromagnetic substances.

1.13.3. Paramagnetism

There are unpaired electrons in a paramagnetic material, i.e., atomic or molecular orbitals which contain exactly one electron. While the Pauli Exclusion Principle allows paired electrons to have their intrinsic (spin) magnetic moments pointed in opposite directions, causing the cancelation of their magnetic fields, an unpaired electron is free to align its magnetic moment in any direction. When an external magnetic field is applied, certain magnetic moments tend to align in the same direction as the field being applied, thus increasing it.

1.13.4. Ferromagnetism

A ferromagnet has unpaired electrons, as a paramagnetic element. Nevertheless, in addition to the tendency of the intrinsic magnetic moment of the electrons to be parallel to an applied field, there is also a tendency in these materials to align themselves parallel to each other in order to maintain a lower-energy state. Thus the magnetic moments of the electrons in the material are naturally aligned parallel to each other even in the absence of an applied field. Each ferromagnetic material has its temperature over which it loses its ferromagnetic properties, called the Curie temperature, or Curie point. This is because the thermal tendency to disorder overwhelms the energy-lowering due to ferromagnetic order. Ferromagnetism only occurs in a few substances; the common ones are iron, nickel, cobalt, their alloys, and some alloys of rare earth metals.

1.13.5. Magnetic Domain

In a ferromagnetic substance the magnetic moments of atoms cause them to behave something like tiny permanent magnets. They hold together and align with small, more or less uniformly aligned regions called magnetic domains or Weiss domains. With a magnetic force microscope, magnetic domains can be examined to reveal magnetic domain boundaries which resemble the white lines in the illustration. Many scientific experiments can exhibit magnetic fields physically. When a domain contains too many molecules, it becomes unstable and splits into two domains aligned in opposite directions, so that they remain more stable together as shown at the right. The domain boundaries change when exposed to a magnetic field, so that the domains associated with the magnetic field expand and dominate the structure (pointed yellow area),

as shown on the left. When removing the magnetizing field the domains may not return to an un-magnetized state.

It results in the magnetizing of the ferromagnetic substance, which forms a permanent magnet.

The substance is magnetically saturated when magnetized strongly enough that the regular domain overruns all other domains to result in only one single domain. This domain alignment structure returns spontaneously when the substance is cooled, in a way that is roughly analogous to how a liquid would freeze into a crystalline solid.

1.13.6. Anti-ferromagnetism

An anti-ferromagnet, unlike a ferromagnet, tends to point in opposite directions for the intrinsic magnetic moments of adjacent valence electrons. The material is antiferromagnetic when all atoms are structured in a product in such a way that each neighbour is anti-aligned. Anti-ferromagnetism has a net magnetic moment of zero, meaning that they do not generate any field. Anti-ferromagnet is less common compared to other type of behavior and is mostly observed at low temperatures. Anti-ferromagnetism can be seen to have diamagnetic and ferromagnetic properties at varying temperatures. Opposing electrons in some materials want to move in opposite directions, but there is no geometrical structure in which each opposing pair is anti-aligned. This is called a spin glass and is an example of frustration with geometry.

1.13.7. Ferrimagnetism

As with ferromagnetism, ferrimagnets in the absence of a field maintain their magnetization. Neighbouring pairs of electron spins, however, tend to point in opposite directions, like antiferromagnetic materials.

These two properties are not contradictory as there is a more magnetic moment from the sub lattice of electrons pointing in one direction, in the optimal geometrical arrangement, than from the sub lattice pointing in the opposite direction.

Most ferrites are of ferromagnetic nature. The first magnetic substance discovered magnetite, is a ferrite, and was originally thought to be a ferromagnet;

However, after seeing ferromagnetism, Louis Neel disproved this.

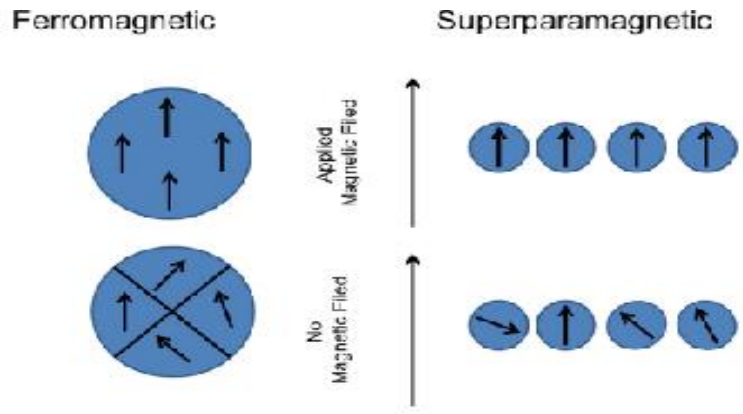

Figure 1.14. Ferromagnetic and super paramagnetic.

1.13.8. Superparamagnetism

The material is super paramagnetic if made of tiny non-interacting magnetic grains of a single domain distributed in some non-magnetic medium. How weak it is, depends on the magnetic grain properties. A Typical diameter value is in the order of 10 nm. Since the features of super paramagnetic materials depend crucially on the magnetic grain spontaneous moment, it is implicitly understood that the temperature of magnetic grains is below the Curie or Neel temperature T_C. Talking about super paramagnetism over T_C doesn't make sense. When a ferromagnet or ferrimagnets is sufficiently small, it acts like a single magnetic spin that is subject to Brownian motion. Its response to a magnetic field is qualitatively similar to the reaction of a paramagnet but much more significant.

(A) Applications

Information is stored in hard disk drives by magnetizing small pieces of magnetic material onto the platter. The former contains magnetic nano grains. Ferrofluids, which are a colloidal liquid with magnetic nanoscale grains suspended in a carrier liquid, are used in liquid seals (e.g. in HDDs), efficient heat transfer (e.g. in loudspeakers), in suspension systems and in various medical applications. They also look nice when a permanent magnet is put in the vicinity.

1.14. Aim of study

The use of electronic devices (mobiles, camera, computers, Television, etc.) now a day is more demanding the continuous improvement in miniaturization of these devices. The memory and energy storage devices are demanding high dielectric constant and low loss materials scientist taking interest regarding better to serve these microelectronic devices.

(i) The work focuses synthesis characterization and application of dielectric, ferroelectric, and magnetic properties of materials and its dependence on temperature as well as frequency. Effect of sintering duration on composite and its effect on dielectric, and electrical properties.

(ii) Separate contribution of grain and grain boundary, microstructure, particle shape, temperature and frequency on the dielectric, and electric properties are widely studied.

(iii) To get good quality of ceramic materials solid state method and semi-wet route are used to monitor homogeneous mixing of metal ions and material synthesized at low sintering temperature as well as less duration. To get high dielectric constant and low dielectric loss the synthesized materials Mn-dope CCTO are use as capacitor and memory storage devices.

The objective of present work is to synthesize following ceramic material and composite of various metal ions at some concentrations

1. $CaCu_3Ti_4MnO_{12}$ synthesized through semi-wet route
2. $CaCu_3Ti_{3.5}Mn_{0.5}O_{12}$ synthesized through semi-wet route
3. $CaCu_3Ti_{3.75}Mn_{0.25}O_{12}$ synthesized through semi-wet route
4. $CaCu_3Ti_{3.5}W_{0.5}O_{12}$ synthesized through semi-wet route
5. $CaCu_3Ti_{3.5}Nb_{0.5}O_{12}$ synthesized through semi-wet route

Characterizations of the sample were carried out by different physiochemical methods by the following sequential steps:

i. Study the crystal structure and single phase formation of the ceramic compositions using X-ray powder diffraction
ii. Study of the surface morphology using Scanning Electron Microscopy (SEM)
iii. Determination of particle size by Transmission Electron Microscopy (TEM).
iv. Investigation of dielectric properties as a function of temperature as well as frequency.
v. Besides, a correlation between dielectric behavior and those of microstructure and defect structure will also be established.
vi. Rationalization of dielectric properties by impedance and modulus spectroscopic studies
vii. Study of AC conductivity as a function of temperature and frequency to investigate the mechanism of conduction.

Different physiochemical techniques will characterize these ceramic. The powder X-ray diffraction will be recorded to study the crystal structure and single phase formation of the ceramic. Scanning electron micrographs of the ceramics will be recorded to study the surface morphology, and transmission electron micrographs will be obtained to determine their particle size. The purity and stoichiometry of each of grain and their grain boundary region will be assessed by the energy dispersive X-ray studies.

To obtain high dielectric constant and low dielectric loss ceramic, the dielectric and electrical properties will be studied as a function of temperature as well as frequency. In addition, a correlation between dielectric behavior and those of microstructure and defect structure will also be established.

1.14.1. Applications of Perovskites

Perovskites materials	**APPLICATION**
$BaTiO_3$	Multilayer Capacitor [Park (2005)]
Pb $(Zr_xTi_{1-x})O_3$	Piezoelectric Transducer [Lendermann *et al.* (2004)]
$BaTiO_3$	P. T. C. Thermistor [Affleck and Leach (2005)]
(Pb, La) $(Zr, Ti)O_3$	Electrooptical Modulator [Nakada*et al.* (2003)]
$BaZrO_3$	Dielectric Resonator [Shi (2008)]
Pb $(Mg_{1/3}\ Nb_{2/3})O_3$	Elecrostrictive Actuator [Takagi *et al.* (1993)]
Ba (Pb, Bi)O_3 layered cuprates	Superconductor [Grumann *et al.* (1994)]
$GdFeO_3$	Magnetic Bubble Memory [Kanta and Kumar (2014)]
$YAlO_3$	Laser Host [Belt *et al.* (2003)]
(Ca, La)MnO_3	Ferromagnet [Heffner *et al.* (2000)]
$SrCeO_3$ $BaZrO_3$	Hydrogen sensor [Iwarahae*t al.* (1981)] H_2 production/ extraction **[**Iwarahae*t al.* (1988)]
(La, Sr) (Ga, Mg)$O_{3\delta}$	Solid electrolyte [Yamanaka *et al.* (2003)]

[1] Clarke, D. R. (1987). Grain boundaries in polycrystalline ceramics. *Annual Review of Materials Science*, **17**(1), 57-74.

[2] Megaw, H. D. (1946). Crystal structure of double oxides of the perovskite type. *Proceedings of the Physical Society*, **58**(2), 133.

[3] Wood, E. A. (1951). Polymorphism in potassium niobate, sodium niobate, and other ABO_3 compounds. *Acta Crystallographica*, **4**(4), 353-362.

[4] Keith, M. L., & Roy, R. (1954). Structural relations among double oxides of trivalent elements.*American Mineralogist*, **39**(1-2), 1-23.

[5] Roth, R. S. (1957). Classification of perovskite and other ABO_3-type compounds. *J. Res. Nat. Bur. Stand*, ***58***(2), 75-88

[6] Yakel, H. L. (1955). On the structures of some compounds of the perovskite type. *Acta Crystallographica*, ***8***(7), 394-398

[7] Galasso, F. S. (2013). *Structure, properties and preparation of perovskite-type compounds: international series of monographs in solid state physics* (Vol. 5). Elsevier.

[8] Matthias, B. T. (1949). Ferro-electric Properties of W O 3. *Physical Review*, *76*(3), 430.

[9] Fouskova, A., & Cross, L. E. (1970).Dielectric properties of bismuth titanate. *Journal of Applied Physics*, **41**(7), 2834-2838.

[10] Shao, S. F., Zhang, J. L., Zheng, P., & Wang, C. L. (2007).Effect of Cu-stoichiometry on the dielectric and electric properties in $CaCu_3Ti4$ O 12 ceramics. *Solid state communications*, **142**(5), 281-286.

[11] Rai, A.K., Mandal, K.D., Kumar, D., &Parkash, O. (2009). Dielectric properties of lanthanum-doped $CaCu_3Ti_4O_{12}$ synthesized by semi-wet route. *Journal of Physics and Chemistry of Solids*, **70**(5), 834-839

[12] Prakash, B. S., &Varma, K. B. R. (2006). Microstructural and dielectric properties of donor doped (La^{3+}) $CaCu_3Ti_4O12$ ceramics. *Journal of Materials Science: Materials in Electronics*, **17**(11), 899-90

[13] Parkash, O., Kumar, D., Goyal, A., Agrawal, A., Mukherjee, A., Singh, S., & Singh, P. (2008). Electrical behaviour of zirconium doped calcium copper titanium oxide. *Journal of Physics D: Applied Physics*, **41**(3), 035401.

[14] Mandal, K. D., Rai, A. K., Kumar, D., &Parkash, O. (2009). Dielectric properties of the $Ca_{1-x}La_xCu_3Ti_{4-x}Co_xO_{12}$ system (x= 0.10, 0.20 and 0.30) synthesized by semi-wet route. *Journal of Alloys and Compounds*, **478**(1), 771-776

[15] Zhi, J., Chen, A., Zhi, Y., Vilarinho, P. M., &Baptista, J. L. (1999).Incorporation of yttrium in barium titanate ceramics.*Journal of the American Ceramic Society*, **82**(5), 1345-134

[16] Prasad, C. D., Parkash, O., & Kumar, D. (1988). Electrical properties of $La_{1-x}Pb_xCo_{1-x}Ti_xO_3$ (x= 0.05 and 0.10). *Journal of materials science letters*, **7**(7), 789-790.

[17] Parkash, O., Pandey, L., Tewari, H. S., Tare, V. B., &Kimar, D. (1990).Dielectric relaxatorbehaviour of $Sr_{0.8}La_{0.2}Ti0.8Co_{0.2}O_3$. *Ferroelectrics*, **102**(1), 203-211

[18] Kumar, A., Dwivedi, R. K., & Pal, V. (2012).Dielectric Behavior and Impedance Spectroscopy of $Ba_{1-x}Bi_xTi_{1-x}Fe_xO_3$ System.In *Advanced Materials Research* (Vol. 585, pp. 190-194).Trans Tech Publications.

[19] Pecharroman, C., Esteban-Betegon, F., Bartolome, J. F., Lopez-Esteban, S., & Moya, J. S. (2001). New Percolative $BaTiO_3$–Ni Composites with a High and Frequency-Independent Dielectric Constant ($\epsilon r \approx 80000$). *Advanced Materials*, **13**(20), 1541-1544.

[20] Ohtsu, N., Sato, K., Yanagawa, A., Saito, K., Imai, Y., Kohgo, T., & Hanawa, T. (2007). $CaTiO_3$ coating on titanium for biomaterial application—Optimum thickness and tissue response.*Journal of Biomedical Materials Research Part A*, **82**(2), 304-315.

[21] Lemanov, V. V., Sotnikov, A. V., Smirnova, E. P., Weihnacht, M., &Kunze, R. (1999). Perovskite $CaTiO_3$ as an incipient ferroelectric. *Solid State Communications*, **110**(11), 611-614.

[22] Müller, K. A., & Burkard, H. (1979). $SrTiO_3$: An intrinsic quantum paraelectric below 4K. *Physical Review B*, **19**(7), 3593.

[23] Sawaguchi, E., & Kikuchi, A. (1962).Dielectric constant of strontium titanate at low temperatures.*Journal of the Physical Society of Japan*, **17**(10), 1666-1667.

[24] De Groot, F. M. F., Grioni, M., Fuggle, J. C., Ghijsen, J., Sawatzky, G. A., & Petersen, H. (1989). Oxygen 1s x-ray-absorption edges of transition-metal oxides. *Physical Review B*, **40**(8), 5715

[25] Lytle, F. W. (1964). X-Ray Diffractometry of Low-Temperature Phase Transformations in Strontium Titanate. *Journal of Applied Physics*, **35**(7), 2212-2215.

[26] Kalkhoran, B. R. (2004). *Microstructural Studies on the Reoxidation Behavior of Nb-doped SrTiO3 Ceramics* (Doctoral dissertation, Dissertation an der Universität Stuttgart).

[27] Cao, L., Sozontov, E., &Zegenhagen, J. (2000). Cubic to Tetragonal Phase Transition of $SrTiO_3$ under Epitaxial Stress: An X-Ray Backscattering Study. *physica status solidi (a)*, **181**(2), 387-404.

[28] Subramanian, M. A., Li, D., Duan, N., Reisner, B. A., & Sleight, A. W. (2000).High dielectric constant in $ACu_3Ti_4O_{12}$ and ACu_3Ti_3 FeO_{12} phases.*Journal of Solid State Chemistry*, **151**(2), 323-325

[29] Löhnert, R., Bartsch, H., Schmidt, R., Capraro, B., &Töpfer, J. (2015). Microstructure and electric properties of $CaCu_3Ti_4O_{12}$ multilayer capacitors. *Journal of the American Ceramic Society*, **98**(1), 141-147

[30] Kretly, L. C., Almeida, A. F. L., De Oliveira, R. S., Sasaki, J. M., & Sombra, A. S. B. (2003). Electrical and optical properties of $CaCu_3Ti_4O_{12}$ (CCTO) substrates for microwave devices and antennas.*Microwave and Optical Technology Letters*, **39**(2), 145-150.

[31] Ponce, M. A., Ramirez, M. A., Schipani, F., Joanni, E., Tomba, J. P., & Castro, M. S. (2015). Electrical behavior analysis of n-type $CaCu_3Ti_4O_{12}$ thick films exposed to different atmospheres. *Journal of the European Ceramic Society*, **35**(1), 153-161.

[32] Sulaiman, M. A., Hutagalung, S. D., Ain, M. F., & Ahmad, Z. A. (2010). Dielectric properties of Nb-doped $CaCu_3Ti_4O_{12}$ electroceramics measured at high frequencies. *Journal of Alloys and Compounds*, **493**(1), 486-492.

[33] Yuan, W. X., Hark, S. K., & Mei, W. N. (2010). Investigation of triple extrinsic origins of colossal dielectric constant in $CaCu_3Ti_4O_{12}$ ceramics. *Journal of The Electrochemical Society*, **157**(5), G117-G120.

[34] Wang, M. H., Zhou, F., Wang, Q. L., & Yao, C. (2012).Synthesis of $CaCu_3Ti_4O_{12}$ powders and ceramics by sol-gel method using decanedioic acid and its dielectric properties. *Journal of Central South University*, *19*(12), 3385-3389.

[35] Banerjee, N., & Krupanidhi, S. B. (2010). Low temperature synthesis of nano-crystalline $CaCu_3Ti_4O_{12}$ through a fuel mediated auto-combustion pathway. *Current Nanoscience*, **6**(4), 432-438.

[36] Li, Menglin, Xiuwen Xu, Yuemin Xie, Ho-Wa Li, Yuhui Ma, Yuanhang Cheng, and Sai-Wing Tsang. (2019) "Improving the conductivity of sol–gel derived NiO_x with a mixed oxide composite to realize over 80% fill factor in inverted planar perovskite solar cells. *Journal of Materials Chemistry A*, 9578-9586.

[37] Huang, X., Jiang, P., & Tanaka, T. (2011).A review of dielectric polymer composites with high thermal conductivity. *IEEE Electrical Insulation Magazine*, **27**(4).

[38] Li, J., Liang, P., Yi, J., Chao, X., & Yang, Z. (2015). Phase formation and enhanced dielectric response of $Y_{2/3}Cu_3Ti_4O_{12}$ ceramics derived from the sol–gel process. *Journal of the American Ceramic Society*, **98**(3), 795-803.

[39] Li, Junwei, Pengfei Liang, Jing Yi, Xiaolian Chao, and Zupei Yang. (2015) Phase formation and enhanced dielectric response of $Y_{2/3}Cu_3Ti_4O_{12}$ ceramics derived from the sol–gel process. *Journal of the American Ceramic Society* ,795-803.

[40] Trivedi, M., Solanki, M. S., & Benjamin, R. S. (2015). Use Of Cu-C-Tio_2 In Dye Sensitized Solar Cell. *International Journal of Scientific & Technology Research*, **4**(7), 135-140.

[41] Sarkar, Arpita, Nam Joong Jeon, Jun Hong Noh, and Sang I Seok. (2014) Well-organized mesoporous TiO_2 photoelectrodes by block copolymer-induced sol–gel assembly for inorganic–organic hybrid perovskite solar cells. *The Journal of Physical Chemistry C* **118**, 16688-16693.

[42] Szwagierczak, D. (2009). Dielectric behavior of $B_i2/3Cu_3Ti_4O_{12}$ ceramic and thick films.*Journal of electroceramics*, **23**(1), 56-61.

[43] Liu, J., Duan, C. G., Yin, W. G., Mei, W. N., Smith, R. W., & Hardy, J. R. (2004). Large dielectric constant and Maxwell-Wagner relaxation in Bi $2/3$ $Cu_3Ti_4O_{12}$.*Physical review B*, **70**(14), 144106.

[44] Subramanian, M. A., Li, D., Duan, N., Reisner, B. A., & Sleight, A. W. (2000).High dielectric constant in $ACu_3Ti_4O_{12}$ and $ACu_3Ti_3FeO_{12}$ phases.*Journal of Solid State Chemistry*, **151**(2), 323-325.

[45] Subramanian, M. A., Li, D., Duan, N., Reisner, B. A., & Sleight, A. W. (2000).High dielectric constant in $ACu_3Ti_4O_{12}$ and $ACu_3Ti_3FeO_{12}$ phases. *Journal of Solid State Chemistry*, **151**(2), 323-325.

[46] McEvoy, M. A., & Correll, N. (2015). Materials that couple sensing, actuation, computation, and communication. *Science*, **347**(6228).

[47] José-Yacamán, M., Rendón, L., Arenas, J., &Puche, M. C. S. (1996). Maya blue paint: an ancient nanostructured material. *Science*, **273**(5272), 223.

[48] Theng, B. K. G. (1982). Clay-polymer interactions: summary and perspectives. *Clays and clay minerals*, **30**(1), 1-10.

[49] Kruis, F. E., Fissan, H., & Peled, A. (1998).Synthesis of nanoparticles in the gas phase for electronic, optical and magnetic applications—a review. *Journal of Aerosol Science*, **29**(5), 511-535.

[50] Zhang, S., Sun, D., Fu, Y., & Du, H. (2003). Recent advances of super hard nanocomposite coatings: a review. *Surface and Coatings Technology*, **167**(2), 113-119.

[51] Birkholz, M., Albers, U., & Jung, T. (2004).Nanocomposite layers of ceramic oxides and metals prepared by reactive gas-flow sputtering. *Surface and Coatings Technology*, **179**(2), 279-285.

[52] Shirane, G., Hoshino, S., & Suzuki, K. (1950). X-ray study of the phase transition in lead titanate. *Physical Review*, **80**(6), 1105.

[53] Pilgrim, S. M., Sutherland, A. E., & Winzer, S. R. (1990). Diffuseness as a useful parameter for relaxor ceramics. *Journal of the American Ceramic Society*, **73**(10), 3122-3125.

[54] Ramirez, A. P., Subramanian, M. A., Gardel, M., Blumberg, G., Li, D., Vogt, T., & Shapiro, S. M. (2000).Giant dielectric constant response in a copper-titanate.*Solid State Communications*, **115**(5), 217-220.

[55] Almeida, A. F. L., De Oliveira, R. S., Góes, J. C., Sasaki, J. M., Souza Filho, A. G. D., Mendes Filho, J., &Sombra, A. S. B. (2002). Structural properties of $CaCu_3Ti_4O_{12}$ obtained by mechanical alloying.*Materials Science and Engineering: B*, **96**(3), 275-283.

[56] Moriya, Y., Kawaji, H., Tojo, T., &Atake, T. (2003). Low Temperature Heat Capacity and Dielectric Relaxation in CaCu~ 3Ti~ 4O~ 1~ 2 Ceramics. *TRANSACTIONS-MATERIALS RESEARCH SOCIETY OF JAPAN*, **28**(1), 137.

[57] Lines, M. E., & Glass, A. M. (1977).Principles and applications of ferroelectrics and related materials. Oxford university press.

[58] Waku, S. (1971). Classification and dielectric characteristics of the boundary layer ceramic dielectrics (BL dielectrics). *Rev Elect Commun Lab*, 665-679.

[59] Reaney, I. M., &Ubic, R. (2000).Talking microwaves: A review of ceramics at the heart of the telecommunications network.*Int. Ceram*, **1**, 48-52.

[60] Rauch, W., Gornik, E., Sölkner, G., Valenzuela, A. A., Behner, H., & Gieres, G. (1994). High temperature superconducting coplanar and epitaxially grown microstrip transmission lines studied by a half-wavelength resonator technique. *Applied superconductivity*, **2**(6), 417-423.

[61] Stinton, D. P., & Richerson, D. W. (1992). *Low-expansion ceramics initiative* (No. CONF-9211101-9). Oak Ridge National Lab., TN (United States).

[62] Weiler, K. W., & Seielstad, G. A. (1971). Synthesis of the Polarization Properties of 3C 10 and 3C 58 at 1420 and 2880 MHz. *The Astrophysical Journal*, **163**, 455-478.

[63] Chen, H., Cong, T. N., Yang, W., Tan, C., Li, Y., & Ding, Y. (2009). Progress in electrical energy storage system: A critical review. *Progress in Natural Science*, **19**(3), 291-312.

[64] Asami, K. (2002). Characterization of heterogeneous systems by dielectric spectroscopy.*Progress in polymer science*, **27**(8), 1617-1659.

[65] Newnham, R. E. (1983). Structure-property relations in ceramic capacitors.*J Mater Educ*, **5**, 947-82.

[66] Barsukov, Y., & Macdonald, J. R. (2012). Electrochemical impedance spectroscopy. *Characterization of materials*, **2**, 898-913.

[67] Schmidt, R., Eerenstein, W., Winiecki, T., Morrison, F. D., & Midgley, P. A. (2007). Impedance spectroscopy of epitaxial multiferroic thin films. *Physical Review B*, **75**(24), 245111.

[68] Adams, T. B., Sinclair, D. C., & West, A. R. (2002). Giant barrier layer capacitance effects in $CaCu_3Ti_4O_{12}$ ceramics. *Advanced Materials*, **14**(18), 1321-1323.

[69] Irvine, J. T., Sinclair, D. C., & West, A. R. (1990).Electroceramics: characterization by impedance spectroscopy. *Advanced Materials*, **2**(3), 132-138.

[70] Jaber, I. S., & Ahmed, M. R. (2004). Technical and economic evaluation of brackish groundwater desalination by reverse osmosis (RO) process. *Desalination*, **165**, 209-213.

[71] Odom, B., Hanneke, D., d'Urso, B., & Gabrielse, G. (2006). New measurement of the electron magnetic moment using a one-electron quantum cyclotron. *Physical review letters*, **97**(3), 030801.

[72] Osman, K. I. (2011). Synthesis and characterization of $BaTiO_3$ ferroelectric material.

[73] Luo, S. N., Ahrens, T. J., & Asimow, P. D. (2003). Polymorphism, superheating, and amorphization of silica upon shock wave loading and release. *Journal of Geophysical Research: Solid Earth*, **108** (B9).